Safe PDE Backstepping QP Control With High Relative Degree CBFs: Stefan Model With Actuator Dynamics

Shumon Koga , *Member, IEEE*, and Miroslav Krstic , *Fellow, IEEE*

Abstract—**High-relative-degree control barrier functions play a prominent role in automotive safety and in robotics. In this article, we launch a generalization of this concept for PDE control, treating a specific, physically relevant model of thermal dynamics where the boundary of the PDE moves due to a liquid–solid phase change—the so-called Stefan model. The familiar quadratic programming (QP) design is employed to ensure safety but with CBFs that are infinite-dimensional (including one control barrier "functional") and with safe sets that are infinite-dimensional as well. Since, in the presence of actuator dynamics, at the boundary of the Stefan system, this system's main CBF is of relative degree 2, an additional CBF is constructed, by backstepping design, which ensures the positivity of all the CBFs without any additional restrictions on the initial conditions. It is shown that the "safety filter" designed in this article guarantees safety in the presence of an arbitrary operator input. This is similar to an automotive system in which a safety feedback law overrides—but only when necessary—the possibly unsafe steering, acceleration, or braking by a vigorous but inexperienced driver. Simulations have been performed for a process in metal additive manufacturing, which show that the operator's heat-and-cool commands to the Stefan model are being obeyed but without the liquid ever freezing.**

Index Terms—**Additive manufacturing (AM), control barrier function (CBF), distributed parameter systems, nonlinear control, quadratic program, safety, Stefan problem.**

I. INTRODUCTION

A. Safety, Hi-Rel-Deg CBFs, and Nonovershooting Control

GUARANTEED safety is a necessity in most engineering applications, including robotic and automotive systems.

Several approaches have been developed for ensuring safety, such as reachability analysis [4], contraction theory [41], model predictive control [17], and so on. Since the seminal work on control barrier functions (CBFs) [2], CBF-based designs for safety have garnered tremendous attention. While they come with Lyapunov-like characterizations, CBFs are actually system outputs, which need to be kept positive. An alternative perspective is that keeping those inputs positive ensures that a certain desired set is positively/forward-invariant for the system.

The introduction of high-relative-degree (hi-rel-deg) CBFs in 2016 [38], and their further nonlinear refinement [44], constitute breakthroughs in removing the relative degree 1 restriction of the early CBF work. Much progress has followed, including [5], [11], [20], [45], to mention a few.

While not called "high-relative-degree CBFs" (or CBFs at all), they do first appear in the second author's 2006 article [32], ten years prior to [38]. In that article [32], for a class of nonlinear systems, the so-called "nonovershooting control" problem is solved, as one form of safety used to be referred to in the earlier literature, particularly for setpoint regulation of outputs of linear plants without exceeding the setpoint.

B. Safe Control for PDEs

Control with safety guarantees plays a prominent role in robotics and in collision avoidance for autonomous vehicles. For PDEs, i.e., in infinite dimension, safe control has appeared only where the infinite-dimensional state needs to maintain a positive value for reasons of physical validity of the model, such as when the state is distributed concentration [19] or gas density [21], or when the liquid level must be kept below a certain value to avoid spilling [22].

This article makes a significant advance to this inquiry—PDE safety. We consider a thermal system, known as the Stefan PDE–ODE system, which models a solid–liquid phase change and whose liquid needs to be kept from developing islands of solid in its midst, while an operator is pursuing his objective which may, for example, be the relocation of the liquid–solid interface to a desired position.

While we did achieve in [24] the result of regulating the interface to a setpoint while maintaining the entire liquid in that phase, we had done that using direct actuation of the heat flux at the liquid boundary. Realistic actuation does not have direct access to heat flux but is performed with an electrical actuator

whose input is voltage connected to the heater through RC series circuit. In other words, the input for which a controller was designed in [24] and the realistic voltage input are separated by at least an integrator. This addition of an integrator changes the meaning of safety for the Stefan model. Even though just a single state variable has been added to a model of infinite dimension, the dimension did increase by one and with that the geometry of the safe set that needs to be maintained forward invariant changes. An alternative perspective is that, with the addition of an integrator, the relative degrees of the CBFs for the Stefan system have increased by one.

Hence, a nontrivial modification to the feedback in [24] is needed in order to retain what has been achieved there but in the presence of an integrator at the input. This retention of safety is accomplished by suitably employing, and extending, the backstepping design idea for safety from [32].

C. QP Modifications for Stefan PDE and Actuator ODE

This article differs from [19], [21], and [22] not only in the sense of the physics considered—thermal here and bio-populations, gas dynamics, and free-surface flows in those papers. Another difference is that what was achieved safely in those papers is stabilization, whereas in this article, we tackle a more general objective of safeguarding the system from the potentially unsafe input being applied by an external operator—similar to safeguarding a vehicle, using dynamic stability control, from the unsafe, overly aggressive actions of an inexperienced driver who does not have a good feel for his car's dynamics. We let the operator manipulate the input voltage to the liquid–solid system for as long as his inputs will not create solid islands in the liquid. But for inputs that would violate the phase change constraints, we override the operator with a feedback law that guarantees safety.

This safety override is performed by a quadratic programming (QP)-feedback modification of the nominal input. Since this QP modification relies on a backstepping transformation to introduce a CBF of relative degree 1 to which QP can be applied, we call this a "QP-backstepping-CBF" design.

In the Stefan model with actuator dynamics, we have two CBFs: one of relative degree 1 representing the heat flux at the boundary, which must be maintained positive so that the temperature of the liquid remains above freezing and the conditions of the "maximum principle" for the heat PDE are met, and the second CBF that is of relative degree 2 and incorporates the position of the liquid–solid interface and the deviation of the actual temperature from the freezing temperature. A single input must keep both of these CBFs positive. This is achieved by two QP modifications, which, when combined, give a physically natural feedback that saturates the operator's command between two safety feedback laws, one ensuring that the system is heated enough and the other ensuring that it is not overheated.

D. Stefan Model of Phase Change and Its Control

The Stefan model of the liquid–solid phase change has been widely utilized in various kinds of science and engineering processes, including sea-ice melting and freezing [26], continuous casting of steel [39], cancer treatment by cryosurgeries [40], additive manufacturing (AM) [29], crystal growth [14], and thermal energy storage systems [30]. Apart from the thermo-dynamical model, the Stefan PDE–ODE systems have been employed to model several chemical, electrical, social, and financial dynamics, such as lithium-ion batteries [23], tumor growth process [15], neuron growth [10], domain walls in ferroelectric thin films [36], spreading of invasive species in ecology [12], information diffusion on social networks [43], and the American put option [7].

To the best of our knowledge, efforts on control of the Stefan problem on the full PDE–ODE model commence with the motion planning results in [18] and [13]. Approaches employing finite-dimensional approximations are [3] and [9]. For control objectives, infinite-dimensional approaches have been used for stabilization of the temperature profile and the moving interface of a 1-D Stefan problem, such as enthalpy-based feedback [39] and geometric control [35]. These works designed control laws ensuring the asymptotical stability of the closed-loop system in the L_2 norm. However, the results in [35] are established based on the assumptions of the liquid temperature being greater than the melting temperature, which must be ensured by showing the positivity of the boundary heat input.

Recently, boundary feedback controllers for the Stefan problem have been designed via a "backstepping transformation" [31], [33], [42], which has been used for many other classes of infinite-dimensional systems. For instance, Koga et al. [24] designed a state feedback control law, an observer design, and the associated output feedback control law by introducing a nonlinear backstepping transformation for moving boundary PDE, which achieved exponential stabilization of the closed-loop system without imposing any a priori assumption, with ensuring the robustness with respect to the parameters' uncertainty. Numerous other results can be found in [27]. However, the notion of safety and CBFs has not been treated in PDE systems, let alone for the Stefan system.

E. Results and Contributions of the Article

This article develops two safe control designs for the Stefan PDE–ODE system with actuator dynamics by employing the CBF technique. As remarked in Section I-C, three CBFs are considered, two of which are given by the physical restrictions in the Stefan model, and the other one is designed to deal with a CBF with relative degree 2. First, we develop a nonovershooting control to regulate the liquid–solid interface position at a set-point position, with satisfying the positivity of all CBFs. Next, we design a QP-backstepping-CBF of safety filter for a given nominal or operator input, with ensuring that the closed-loop system satisfies the positivity of all CBFs. Then, revisiting the nonovershooting control, the global exponential stability of the closed-loop system is proven via the PDE-backstepping and Lyapunov method. This article extends our conference paper [28] by

1) developing the safe control under the additional constraints from above on states via both nonovershooting and QP control;
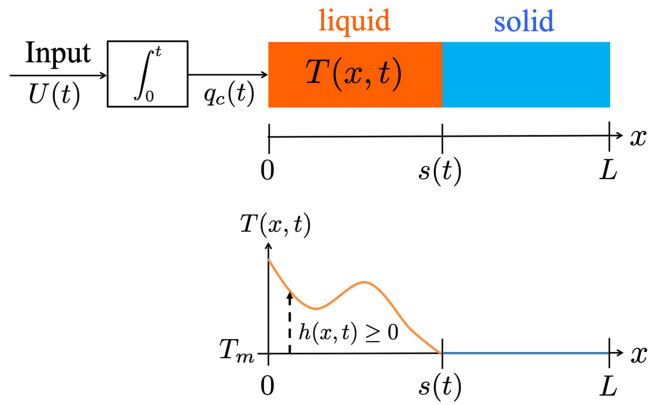
Fig. 1. Schematic of the one-phase Stefan problem with actuator dynamics.

2) deriving the nonovershooting regulation for the Stefan system with a general higher order actuator dynamics;
3) ensuring the safety constraints for the two-phase Stefan system that incorporates the dynamics of the solid phase with a disturbance under the nonovershooting control;
4) applying the two safe control methods to a process in metal AM of a titanium alloy through numerical simulation.

F. Organization

The rest of this article is organized as follows. The one-phase Stefan model with actuator dynamics of the first order and its state constraints are provided in Section II. The nonovershooting regulation is derived in Section III, and a QP-backstepping safety filter is designed in Section IV, with providing the theorem. The stability analysis under the nonovershooting regulation is given in Section V. The safe control under the additional constraints from above on states is developed in Section VI, and the nonovershooting regulation for a higher order actuator dynamics is shown in Section VII. The two-phase Stefan problem with unknown disturbance is presented in Section VIII. The application to metal AM is presented in Section IX. Finally, Section X concludes this article.

Notation and definitions: Throughout this article, partial derivatives and the positive definite functional are denoted as $u_t(x,t) = \frac{\partial u}{\partial t}(x,t)$, $u_x(x,t) = \frac{\partial u}{\partial x}(x,t)$, and $\|u[t]\| = \sqrt{\int_0^{s(t)} u(x,t)^2 dx}$, where $u[t]$ is a function defined on $[0, s(t)]$ with real values defined by $(u[t])(x) = u(x,t)$ for all $x \in [0, s(t)]$. $\mathbb{R}_+ := [0, +\infty)$. $C^0(U; \Omega)$ is the class of continuous mappings on $U \subseteq \mathbb{R}^n$, which takes values in $\Omega \subseteq \mathbb{R}$ and $C^k(U; \Omega)$, where $k \geq 1$ is the class of continuous functions on U, which have continuous derivatives of order k on U and takes values in Ω.

II. STEFAN MODEL AND CONSTRAINTS

Consider the melting or solidification in a material of length L in one dimension (see Fig. 1). Divide the domain $[0, L]$ into two time-varying subintervals: $[0, s(t)]$, which contains the liquid phase, and $[s(t), L]$, that contains the solid phase. Let heat flux enter at boundary $x = 0$, which affects the distal liquid–solid interface dynamics through heat propagation across the liquid phase. Evidently, the heat equation alone does not completely describe the phase transition and must be coupled with the dynamics of the moving boundary.

The energy conservation and heat conduction laws yield the heat equation of the liquid phase, the boundary conditions, and the initial values as follows:

$$T_t(x,t) = \alpha T_{xx}(x,t), \quad \text{for } t > 0, \ 0 < x < s(t) \quad (1)$$

$$-kT_x(0,t) = q_c(t), \quad \text{for } t > 0 \quad (2)$$

$$T(s(t),t) = T_m, \quad \text{for } t > 0 \quad (3)$$

$$s(0) = s_0, \text{ and } T(x,0) = T_0(x), \text{for } x \in (0, s_0] \quad (4)$$

where $\alpha := \frac{k}{\rho C_p}$, and $T(x,t)$, $q_c(t)$, ρ, C_p, and k are the distributed temperature of the liquid phase, the boundary heat flux, the liquid density, the liquid heat capacity, and the liquid heat conductivity, respectively.

In this article, we model the heater, which produces the heat flux $q_c(t)$, as actuated by an input voltage $U(t)$ of a linear *RLC*-network through a nonlinear feedback:

$$\dot{q}_c(t) = U(t). \quad (5)$$

The derivation of (5) from the *RC* series circuit and a real voltage input is given in Appendix A. For the sake of readability, hereafter, we call $U(t)$ just as voltage input. The local energy balance at the liquid–solid interface $x = s(t)$ is

$$\dot{s}(t) = -\beta T_x(s(t),t) \quad (6)$$

where $\beta := \frac{k}{\rho \Delta H^*}$ and ΔH^* represents the latent heat of fusion. In (6), the left-hand side represents the latent heat, and the right-hand side represents the heat flux by the liquid phase. As the moving interface $s(t)$ depends on the temperature, the problem defined in (1)–(6) is nonlinear. The temperature in the solid is assumed at melting.

There are two requirements for the validity of the model (1)–(6):

$$T(x,t) \geq T_m \quad \forall x \in (0, s(t)) \ \ \forall t > 0 \quad (7)$$

$$0 < s(t) < L \quad \forall t > 0. \quad (8)$$

First, the trivial: the liquid phase is not frozen, i.e., the liquid temperature $T(x,t)$ is greater than the melting temperature T_m. Second, equally trivially, the material is not entirely in one phase, i.e., the interface remains inside the material's domain. These physical conditions are also required for the existence and uniqueness of solutions [1]. Hence, we assume the following for the initial data.

Assumption 1: $0 < s_0 < L$, $T_0(x) \in C^1([0, s_0]; [T_m, +\infty))$ with $T_0(s_0) = T_m$.

Lemma 1: With Assumption 1, if $q_c(t)$ is a bounded piecewise continuous nonnegative heat function, i.e.,

$$q_c(t) \geq 0 \quad \forall t \geq 0 \quad (9)$$

then there exists a unique classical solution for the Stefan problem (1)–(6), which satisfies (7), and

$$\dot{s}(t) \geq 0 \quad \forall t \geq 0. \tag{10}$$

The definition of the classical solution of the Stefan problem is given in [24, Appendix A]. The proof of Lemma 1 is by maximum principle for parabolic PDEs and Hopf's lemma, as shown in [16].

III. NONOVERSHOOTING REGULATION BY BACKSTEPPING FOR MULTIPLE CBFS

The regulation of the interface $s(t)$ to a desired setpoint s_r is a crucial task in several applications that involve thermal phase change, such as creating a layer of desired thickness in metal AM [29]. However, the actuator dynamics given in (5) introduce a major extra challenge to achieving setpoint regulation while guaranteeing the safety constraints (7), (8).

In this section, we regulate $s(t)$ to s_r, as well as $T(x,t)$ to T_m and q_c to zero. This is an equilibrium at the boundary of the safe set. Such a mix of stabilization and safety control problems is called "nonovershooting control" [32]. In addition to the two physically imposed CBFs, with backstepping we design a third CBF to ensure safety but without having to additionally restrict the initial conditions, which is common in other CBF designs. Such an addition of a CBF, ten years after [32], was independently discovered in the format of hi-rel-deg CBFs in [38]. In the next section, we introduce a "QP-backstepping-CBF design," to allow a safe application of a "nominal feedback," possibly distinct from the setpoint regulating feedback, or an application of an external operator open-loop input, using a QP selection between the nominal input and backstepping-designed safeguards.

Let $h_1(t)$, $\hbar_1(t)$, $h_2(t)$, and $h(x,t)$ be CBFs defined by

$$h_1(t) := \sigma(t)$$
$$= -\left(\frac{k}{\alpha} \int_0^{s(t)} (T(x,t) - T_m)dx + \frac{k}{\beta}(s(t) - s_r) \right) \tag{11}$$

$$\hbar_1(t) = q_c(t) \tag{12}$$

$$h_2(t) = -q_c(t) + c_1\sigma(t) \tag{13}$$

$$h(x,t) = T(x,t) - T_m. \tag{14}$$

The CBF h_1 in (11) represents the "energy deficit" (positive, thermal plus potential) relative to the setpoint equilibrium. The added CBF (13), seemingly redundant because $h_2 = -\hbar_1 + c_1 h_1$, represents a backstepping transformation and is crucial for ensuring that h_1 is maintained positive.

Lemma 2: With Assumption 1, suppose that the following conditions hold:

$$h_1(t) \geq 0 \tag{15}$$

$$\hbar_1(t) \geq 0 \tag{16}$$

for all $t \geq 0$. Then, it holds that

$$h(x,t) \geq 0 \quad \forall x \in (0, s(t)) \quad \forall t \geq 0 \tag{17}$$

$$0 < s_0 \leq s(t) \leq s_r \quad \forall t \geq 0, \tag{18}$$

under the classical solution of (1)–(6).

Lemma 2 is proven with Lemma 1. To validate the conditions (15) and (16) for all $t \geq 0$, at least the conditions must hold at $t = 0$, which necessitate the following assumptions on the initial condition and the setpoint restriction.

Assumption 2: $0 \leq q_c(0)$.

Assumption 3: The setpoint position s_r is chosen to satisfy

$$s_0 + \frac{\beta}{\alpha} \int_0^{s_0} (T_0(x) - T_m)dx \leq s_r < L. \tag{19}$$

Under these assumptions, we perform a design of a regulating control $U(t)$ so that the conditions (15) and (16) hold. Taking the first and second time derivatives of (11), we have

$$\dot{h}_1 = -\hbar_1 = -q_c \tag{20}$$

$$-\ddot{h}_1 = \dot{\hbar}_1 = U. \tag{21}$$

Thus, "energy deficit" CBF defined by (11) has relative degree 2, from the voltage input, according to the perspective in [38], which inherits the backstepping change of variable (13) from [32].

The double integrator $U \mapsto h_1$ is not unlike a model of adaptive/distance cruise control, studied in many papers on CBFs and QP. The single integrator $U \mapsto \hbar_1$ is not unlike a classical (velocity) cruise control problem. Hence, in the Stefan model, achieving safety amounts to simultaneously maintaining safety in terms of both distance and velocity cruise control, without imposing additional restrictions on the initial conditions of the position-like and velocity-like states through design. In addition, in the Stefan model, on top of the two CBFs of relative degrees 1 and 2, one has to maintain the positivity of the CBF (14), i.e., to ensure (17), where the temperature field plays the role of zero dynamics of infinite dimension.

We design a "nonovershooting control" [32], denoted as $U = U^*(\sigma, q_c)$, so that the following relationships hold:

$$\dot{h}_1 = -c_1 h_1 + h_2 \tag{22}$$

$$\dot{\hbar}_1 = -c_1 \hbar_1 + c_2 h_2 \tag{23}$$

$$\dot{h}_2 = -c_2 h_2. \tag{24}$$

Indeed, h_2 in (13) is defined so that (22) holds; hence, it suffices to design the control so that (24) holds. Taking the time derivatives of (13), one gets

$$U^*(\sigma, q_c) = -(c_1 + c_2)q_c + c_1 c_2 \sigma. \tag{25}$$

With (25), we see that (23) also holds.

The solution to the linear differential (22)–(24) is analytically obtained by

$$h_2(t) = h_2(0)e^{-c_2 t} \tag{26}$$

$$h_1(t) = h_1(0)e^{-c_1 t} + \frac{h_2(0)}{c_2 - c_1}(e^{-c_1 t} - e^{-c_2 t}) \tag{27}$$

$$\hbar_1(t) = \hbar_1(0)e^{-c_1 t} + \frac{c_2 h_2(0)}{c_2 - c_1}(e^{-c_1 t} - e^{-c_2 t}). \tag{28}$$

With Assumptions 2 and 3, $h_1(0) \geq 0$ and $\hbar_1(0) \geq 0$ hold. Thus, if $h_2(0) \geq 0$, one can see that the solutions (26)–(28) are all

nonnegative. For $h_2(0) \geq 0$ to hold, we choose the control gain c_1 as

$$c_1 \geq \frac{q_c(0)}{\sigma(0)} \tag{29}$$

and obtain the following lemma.

Lemma 3: Let Assumptions 1–3 hold. Then, the closed-loop system consisting of the plant (1)–(6) with the nonovershooting control law (25), where the gain satisfies (29), guarantees the following to hold:

$$h_1(t) \geq 0, \quad \hbar_1(t) \geq 0, \quad h_2(t) \geq 0 \quad \forall t \geq 0. \tag{30}$$

Moreover, (17) and (18) hold.

We show stability in Section V.

IV. QP-BACKSTEPPING-CBF DESIGN OF SAFETY FILTER

Here, we derive a safety filter to satisfy all CBF constraints for a given operator input. First, we aim to satisfy $h_2 \geq 0$, since it also ensures $h_1 \geq 0$ by the relation of (22), as a designed exponential CBF. Namely, we satisfy

$$\dot{h}_2 \geq -c_2 h_2. \tag{31}$$

Taking the time derivative of (13) and applying (31) leads to the condition of the input as

$$U \leq U^*(\sigma, q_c) \tag{32}$$

where U^* is given in (25). It remains to ensure $\hbar_1 \geq 0$. Since both $h_1 \geq 0$ and $h_2 \geq 0$ are satisfied under the input condition (32), and taking into account the fact that h_2 can be written with respect to h_1 and $\hbar_1$ as defined in (13), we aim to satisfy the following inequality:

$$\dot{\hbar}_1 \geq -\bar{c}_1 \hbar_1 + \bar{c}_2 h_1 \tag{33}$$

for some $\bar{c}_1 > 0$ and $\bar{c}_2 > 0$, which ensures $\hbar_1 \geq 0$. Taking the time derivative of (12), and with (5), to make (33) hold, we arrive at the following condition on the input:

$$U_*(\sigma, q_c) \leq U \tag{34}$$

$$U_*(\sigma, q_c) = -\bar{c}_1 q_c + \bar{c}_2 \sigma. \tag{35}$$

Comparing (25) with (35), for ensuring the feasibility of the two constrains (32) and (34), it is sufficient to choose the gains in accordance with the following conditions:

$$\bar{c}_1 \geq c_1 + c_2, \quad 0 \leq \bar{c}_2 \leq c_1 c_2. \tag{36}$$

By redefining the gain parameters from $(c_1, c_2, \bar{c}_1, \bar{c}_2)$ to $(k_1, k_2, \delta_1, \delta_2)$, one can show that (25) and (35) with the condition (29) are equivalent to the following formulation:

$$U_* = -(k_1 + \delta_1)q_c + k_2 \sigma \tag{37}$$

$$U^* = -k_1 q_c + (k_2 + \delta_2)\sigma \tag{38}$$

where

$$k_1 \geq q_c(0)/\sigma(0), \quad k_2 > 0 \tag{39}$$

$$\delta_1 \geq 0, \quad \delta_2 \geq 0. \tag{40}$$

Finally, a safety filter, for a given nominal or operator input $U_o(t)$, is designed, inspired by [2], by solving the QP problem[1]

$$U = \min_{u \in \mathbb{R}} |u - U_o|^2 \tag{41}$$

$$\text{subject to} \quad U_* \leq u \leq U^*. \tag{42}$$

Applying the Karush–Kuhn–Tucker optimality condition, the explicit solution is

$$U = \min\{\max\{U_*, U_o\}, U^*\}. \tag{43}$$

Since U_* and U^* are designed by backstepping, with an addition of a CBF to given CBFs, we call this safety filter a "QP-backstepping-CBF" design.

The cumbersome formula (43) can be rewritten with a saturation function on the operator input U_o as

$$U = \begin{cases} U^*, & U_o > U^* \\ U_o, & U_* \leq U_o \leq U^* \\ U_*, & U_o < U_*. \end{cases} \tag{44}$$

The analysis and design above establish the following.

Theorem 1: Let Assumptions 1–3 hold. Consider the closed-loop system (1)–(6) with QP safety control (44), (37), and (38), under an arbitrary operator input $U_o(t)$, where the gain parameters are chosen to satisfy (39) and (40). Then, all CBFs defined as (11)–(14) satisfy the constraints $h_1(t) \geq 0, \hbar_1(t) \geq 0$ for all $t \geq 0$, and $h(x, t) \geq 0$ for all $x \in (0, s(t))$ and for all $t \geq 0$.

Note that, if δ_1 and δ_2 are chosen as zero, QP safety control (44) becomes

$$U = U_* = U^* = -k_1 q_c + k_2 \sigma \tag{45}$$

which disregards the operator input U_o and instead performs a nonovershooting regulation to $s = s_r, T = T_m, q_c = 0$, whose stability is proven in the next section.

V. STABILITY OF NONOVERSHOOTING REGULATION

Theorem 2: Let $s(0)$ and $T(x, 0)$ satisfy Assumptions 1–3. Consider the closed-loop system (1)–(6) with the nonovershooting control law (45), where the gain parameters satisfy (39). Then, all CBFs defined as (11)–(14) satisfy the positivity constraints. This means, in particular, that, for all $q_c(0) > 0$, the interface $s(t)$ does not exceed s_r, the temperature $T(x, t)$ does not drop below T_m at any position x between 0 and $s(t)$, and the heat flux $q_c(t)$ never takes a negative value. Furthermore, the closed-loop system is exponentially stable at the equilibrium $s = s_r, T(x, \cdot) \equiv T_m, q_c = 0$, in the sense of the following positive definite functional:

$$\Phi(t) := \|T[t] - T_m\|^2 + (s(t) - s_r)^2 + q_c(t)^2 \tag{46}$$

for all initial conditions in the safe set, i.e., globally. In other words, there exist positive constants $M > 0$ and $b > 0$ such that

---

[1]Strictly speaking, constraints (42) should be written, following the Lie derivative conditions on the CBFs $\hbar_1$ and h_2, as, respectively, $u + \bar{c}_1 \hbar_1 - \bar{c}_2 h_1 \geq 0$ and $-u + c_2 h_2 - c_1 \hbar_1 \geq 0$. But we believe that (42) poses less of a chance to confuse the reader.

the following estimate holds:

$$\Phi(t) \leq M\Phi(0)e^{-bt}. \qquad (47)$$

The safety is already proven in Lemma 3. The rest of this section proves stability in Theorem 2.

Let $X(t)$ be reference error variable defined by $X(t) := s(t) - s_r$. Then, system (1)–(6) is rewritten with respect to $h(x,t)$ defined in (14), $\hbar_1(t)$ defined in (12), and $X(t)$ as

$$s(t) = X(t) + s_r \qquad (48)$$

$$h_t(x,t) = \alpha h_{xx}(x,t) \qquad (49)$$

$$h_x(0,t) = -\hbar_1(t)/k \qquad (50)$$

$$\dot{\hbar}_1(t) = U(t) \qquad (51)$$

$$h(s(t),t) = 0 \qquad (52)$$

$$\dot{X}(t) = -\beta h_x(s(t),t). \qquad (53)$$

A. Backstepping Transformation to Target System

Following [25, Sec. 3.3], we introduce the following forward and inverse transformations:

$$w(x,t) = h(x,t) - \frac{\beta}{\alpha}\int_x^{s(t)} \phi(x-y)h(y,t)\mathrm{d}y$$
$$\qquad - \phi(x-s(t))X(t) \qquad (54)$$

$$\phi(x) = c_1\beta^{-1}x - \varepsilon \qquad (55)$$

$$h(x,t) = w(x,t) - \frac{\beta}{\alpha}\int_x^{s(t)} \psi(x-y)w(y,t)\mathrm{d}y$$
$$\qquad - \psi(x-s(t))X(t) \qquad (56)$$

$$\psi(x) = e^{\bar{\lambda}x}\left(p_1\sin(\omega x) + \varepsilon\cos(\omega x)\right) \qquad (57)$$

where $\bar{\lambda} = \frac{\beta\varepsilon}{2\alpha}$, $\omega = \sqrt{\frac{4\alpha c_1 - (\varepsilon\beta)^2}{4\alpha^2}}$, $p_1 = -\frac{1}{2\alpha\beta\omega}(2\alpha c_1 - (\varepsilon\beta)^2)$, and $0 < \varepsilon < 2\frac{\sqrt{\alpha c_1}}{\beta}$ is to be chosen later. As derived in [25, Sec. 3.3], taking the spatial and time derivatives of (54) along the solution of (49)–(53), and noting the CBF $h_2(t)$ defined in (13) satisfying (24), one can obtain the following target system:

$$w_t(x,t) = \alpha w_{xx}(x,t) + \dot{s}(t)\phi'(x-s(t))X(t) \qquad (58)$$

$$w_x(0,t) = \frac{h_2(t)}{k} - \frac{\beta}{\alpha}\varepsilon\left[w(0,t) - \frac{\beta}{\alpha}\int_0^{s(t)}\psi(-y)w(y,t)\mathrm{d}y\right.$$
$$\left. - \psi(-s(t))X(t)\right] \qquad (59)$$

$$\dot{h}_2(t) = -c_2h_2(t) \qquad (60)$$

$$w(s(t),t) = \varepsilon X(t) \qquad (61)$$

$$\dot{X}(t) = -c_1X(t) - \beta w_x(s(t),t). \qquad (62)$$

Note that (59) is derived using $h_2(t) = -q_c(t) + c_1\sigma(t) = -\hbar_1(t) - c_1(\frac{k}{\alpha}\int_0^{s(t)}(T(x,t)-T_m)\mathrm{d}x + \frac{k}{\beta}(s(t)-s_r)) = -\hbar_1(t) - k(\frac{\beta}{\alpha}\int_0^{s(t)}\phi'(-y)h(y,t)\mathrm{d}y + \phi'(-s(t))X(t))$, with the help of (55). Indeed, the introduction of (13) is part

of the state transformation of $\hbar_1 \to h_2$, and this transformation is complemented by a feedback control given by (25), in order to eliminate U. The objective of the transformation (54) is to add a stabilizing term $-c_1X(t)$ in (62) of the target (w, X)-system, whose stability is easier to prove than that of (u, X)-system.

Note that the boundary condition (61) and the kernel function (55) are modified from the one in [24]. The target system derived in [24] requires $\mathcal{H}_1$-norm analysis for stability proof. However, with the actuation dynamics of the boundary heat input, $\mathcal{H}_1$-norm analysis fails to show the stability. The modification of the boundary condition (61) enables us to prove the stability in L_2 norm, as shown later.

B. Lyapunov Analysis

Following [25, Lemma 20], by introducing a Lyapunov function $V(t)$ defined by

$$V(t) = \frac{1}{2\alpha}\|w[t]\|^2 + \frac{\varepsilon}{2\beta}X(t)^2 \qquad (63)$$

one can see that there exists a positive constant $\varepsilon^* > 0$ such that for all $\varepsilon \in (0, \varepsilon^*)$, the following inequality holds:

$$\dot{V}(t) \leq -bV(t) + \frac{2s_r}{k^2}h_2(t)^2 + a\dot{s}(t)V(t) \qquad (64)$$

where $a = \frac{2\beta\varepsilon}{\alpha}\max\{1, \frac{\alpha c^2 s_r}{2\beta^3\varepsilon^3}\}$, $b = \frac{1}{8}\min\{\frac{\alpha}{s_r^2}, c\}$, and the condition $\dot{s}(t) \geq 0$ ensured in Lemma 1 is applied. We further introduce another Lyapunov function of h_2, defined by

$$V_h(t) = \frac{p}{2}h_2(t)^2 \qquad (65)$$

with a positive constant $p > 0$. Taking the time derivative of (65) and applying (60) yields

$$\dot{V}_h(t) = ph_2\dot{h}_2 = -c_2ph_2(t)^2. \qquad (66)$$

Let $\bar{V}$ be the Lyapunov function defined by

$$\bar{V} = V + V_h. \qquad (67)$$

Applying (64) and (66) with setting $p = \frac{4s_r}{c_2k^2}$, the time derivative of (67) is shown to satisfy

$$\dot{\bar{V}}(t) \leq -\bar{b}\bar{V}(t) + a\dot{s}(t)\bar{V}(t) \qquad (68)$$

where $\bar{b} = \min\{b, 2s_r/k^2\}$. As performed in [25], with the condition $0 < s(t) \leq s_r$ ensured in Lemma 2, the differential inequality (68) leads to

$$\bar{V}(t) \leq e^{as_r}\bar{V}(0)e^{-\bar{b}t} \qquad (69)$$

which ensures the exponential stability of the target system (58)–(62). Due to the invertibility of the transformation (54)–(56), one can show the exponential stability of the closed-loop system, which completes the proof of Theorem 2.

VI. CONSTRAINTS FROM ABOVE ON TEMPERATURE AND HEAT FLUX

A. Upper Bound Constraints

In practical control systems, the capability of the heater is often restricted to a certain range due to the device limitation.

The Stefan problem, as a melting process, is particular in this regard. The heat input should not go beyond a given upper bound, while it is feasible to assume that the lower bound is zero, i.e., the heat actuator does not work as a cooler. Furthermore, the liquid temperature must be lower than some value, which could be the maximum temperature limited by the device or environment for ensuring the safe operation, or the boiling temperature to avoid an evaporation, which is another phase transition, from liquid to gas.

We tackle such an overall state-constrained problem, to guarantee the following conditions to hold:

$$T_{\mathrm{m}} \le T(x,t) \le T^* \quad \forall x \in [0, s(t)] \quad \forall t \ge 0 \tag{70}$$

$$0 \le q_{\mathrm{c}}(t) \le q^* \quad \forall t \ge 0 \tag{71}$$

for some $T^* > T_{\mathrm{m}}$ and $q^* > 0$. First, we state the following lemma for the Stefan problem.

Lemma 4: If $T_m \le T_0(x) \le \Delta \bar{T}_0 (1 - x/s_0) + T_m$ for some $\Delta \bar{T}_0 > 0$, and if $0 \le q_c(t) \le \bar{q}$ holds for some $\bar{q} > 0$ and for all $t \ge 0$, then

$$T_m \le T(x,t) \le \bar{T}(x,t) := K(s(t) - x) + T_m \tag{72}$$

$\forall x \in (0, s(t)) \, \forall t \ge 0$, where $K = \max\{\bar{q}/k, \Delta \bar{T}_0/s_0\}$.

Proof: Let $v(x,t) := \bar{T}(x,t) - T(x,t)$. Taking the time and second spatial derivatives yields

$$v_t = K\dot{s}(t) - T_t(x,t), \quad v_{xx} = -T_{xx}(x,t). \tag{73}$$

Since $0 \le q_c(t)$, we have $\dot{s}(t) \ge 0$. Thus, we obtain

$$v_t \ge \alpha v_{xx} \tag{74}$$

$$v_x(0,t) \le 0, \quad v(s(t),t) = 0. \tag{75}$$

Applying the maximum principle to (74)–(75), we can state that, if $v(x,0) \ge 0$ for all $x \in (0, s_0)$, then $v(x,t) \ge 0$ for all $x \in (0, s(t))$ and all $t \ge 0$, which concludes Lemma 4.

Inspired by Lemma 4, to guarantee that the upper bound constraints (70) and (71) are met, the following assumptions on the initial conditions are imposed.

Assumption 4: $q_c(0) \le \bar{q}_{\mathrm{c}} := \min\{\frac{k}{s_r}(T^* - T_{\mathrm{m}}), q^*\}$.

Assumption 5: $T_m \le T_0(x) \le \Delta \bar{T}_0 (1 - x/s_0) + T_m$, where $\Delta \bar{T}_0 := \frac{s_0}{s_r}(T^* - T_{\mathrm{m}})$.

B. Nonovershooting Regulation

Then, with $h_2(0) \ge 0$, in addition to the positivity of $h_2(t)$, owing to the monotonically decreasing property of (26), it further holds that

$$0 \le h_2(t) \le h_2(0). \tag{76}$$

With this condition, one can see from (23) that

$$0 \le \dot{\hbar}_1 + c_1 \hbar_1 \le c_2 h_2(0). \tag{77}$$

Applying the comparison lemma, the differential inequality (77) leads to the following inequality for the solution:

$$\hbar_1(0)e^{-c_1 t} \le \hbar_1(t) \le \left(\hbar_1(0) - \frac{c_2}{c_1}h_2(0)\right)e^{-c_1 t} + \frac{c_2}{c_1}h_2(0) \tag{78}$$

Considering the lower bound of the left-hand side and the upper bound of the right-hand side, it yields

$$0 \le \hbar_1(t) \le \max\left\{\hbar_1(0), \frac{c_2}{c_1}h_2(0)\right\} \tag{79}$$

and rewriting it as

$$0 \le \hbar_1(t) \le \max\left\{\hbar_1(0), \frac{c_2}{c_1}\left(c_1 h_1(0) - \hbar_1(0)\right)\right\} \tag{80}$$

the following condition for the control gain:

$$c_2 \le \frac{c_1 \bar{q}_{\mathrm{c}}}{c_1 \sigma(0) - q_{\mathrm{c}}(0)} \tag{81}$$

where the right-hand side is positive because of (29) and where $\bar{q}_{\mathrm{c}}$ is defined in Assumption 4, guarantees that

$$0 \le \hbar_1(t) \le \bar{q}_{\mathrm{c}}. \tag{82}$$

Theorem 3: Let $s(0), T(x,0)$, and $q_{\mathrm{c}}(0)$ satisfy Assumptions 1–5. Consider the closed-loop system (1)–(6) with the nonovershooting control law (25), where the gain parameters satisfy (29) and (81). Then, all CBFs defined as (11)–(14) satisfy the positivity constraints, and $\hbar_1 \le \bar{q}_{\mathrm{c}}$ also holds. This means, in particular, that, for all $q_{\mathrm{c}}(0) > 0$, the interface $s(t)$ does not exceed s_{r}, the temperature $T(x,t)$ does not drop below T_{m} and does not exceed the upper limit $T^* > T_{\mathrm{m}}$ at any position x between 0 and $s(t)$, and the heat flux $q_{\mathrm{c}}(t)$ never takes a negative value and does not exceed the upper limit q^*. Furthermore, the closed-loop system is exponentially stable at the equilibrium $s = s_{\mathrm{r}}, T(x,\cdot) \equiv T_{\mathrm{m}}, q_{\mathrm{c}} = 0$, in the sense of the positive definite functional defined as (46), for all initial conditions in the safe set, i.e., globally. In other words, there exist positive constants $M > 0$ and $b > 0$ such that the estimate (47) holds.

The safety is already proven in this section. The stability proof is identical to the derivation in Section V.

C. QP-Backstepping-CBF Design

We also design QP safety filter to ensure the upper bounds. In addition to the QP constraint on input in Section IV, to ensure the upper bound of $\hbar_1$, we introduce another CBF

$$\hbar_1^*(t) = \bar{q}_{\mathrm{c}} - \hbar_1(t). \tag{83}$$

We set out to design QP to satisfy further

$$\dot{\hbar}_1^* \ge -c_1^* \hbar_1^* \tag{84}$$

for some $c_1^* > 0$, which leads to the condition

$$U \le c_1^*(\bar{q}_{\mathrm{c}} - \hbar_1(t)). \tag{85}$$

Thus, by setting $c_1^* = k_1$, we reformulate the upper bound of the control in (38) as

$$U^* = -k_1 q_c + \max\{(k_2 + \delta_2)\sigma, k_1 \bar{q}_{\mathrm{c}}\} \tag{86}$$

We state the following theorem.

Theorem 4: Let Assumptions 1–5 hold. Consider the closed-loop system (1)–(6) with QP safety control (44), (37), and (86), under an arbitrary operator input $U_o(t)$, where the gain parameters are chosen to satisfy (39) and (40). Then, all CBFs defined as (11)–(14) and (83) satisfy the constraints $h_1(t) \ge 0$,

$\hbar_1(t) \geq 0$, and $\hbar_1^*(t) \geq 0$ for all $t \geq 0$. Moreover, all of (70), (71), and (18) hold.

VII. NONOVERSHOOTING REGULATION TO s_r UNDER HIGHER ORDER ACTUATOR DYNAMICS

This section presents how the proposed approach can be applicable to the Stefan system with the higher order actuator dynamics. We consider the nth order actuator dynamics, i.e., n chain of integrator in the actuation path:

$$q_c(t) = p_1(t) \tag{87}$$

$$\dot{p}_i(t) = p_{i+1}(t) \quad \forall i = 1, \ldots, n-1 \tag{88}$$

$$\dot{p}_n(t) = U(t) \tag{89}$$

where $p_i(t)$ for $i \in \{1, \ldots, n\}$ are additional state variables of higher order derivatives of the heat flux, and $U(t)$ is given as the input of the nth order derivative of the heat flux.

With the nth order actuator dynamics, the CBFs for the energy deficit $h_1(t) = \sigma(t) \geq 0$ are denoted as $h_i(t)$ for all $i \in \{1, \ldots, n\}$ since the relative degree of σ is now n, and the CBFs for the heat flux $q_c(t) \geq 0$ are denoted as $\hbar_1 = q_c(t)$ and $\hbar_i(t)$ for $i \in \{1, \ldots, n-1\}$ for additionally constructed CBFs since the relative degree of $q_c(t)$ is now $n-1$. Regarding the relation of the CBFs, we state the following lemma.

Lemma 5: Suppose that it holds

$$\dot{h}_i = -c_i h_i + h_{i+1} \quad \forall i \in \{1, \ldots, n\} \tag{90}$$

$$\dot{h}_{n+1} = -c_{n+1} h_{n+1}. \tag{91}$$

Let $\hbar_i$ for $i \in \{1, \ldots, n\}$ be defined by

$$\hbar_1 = -\dot{h}_1 \tag{92}$$

$$\dot{\hbar}_i = -c_i \hbar_i + \hbar_{i+1} \quad \forall i \in \{1, \ldots, n-1\}. \tag{93}$$

Then, it holds that

$$\hbar_i = -\dot{h}_i \quad \forall i \in \{1, \ldots, n\} \tag{94}$$

$$\dot{\hbar}_n = -c_n \hbar_n + c_{n+1} h_{n+1}. \tag{95}$$

Proof: First, we show (94) by induction. Clearly, it holds for $i = 1$ from (92). Suppose it holds for $i = j$, i.e., $\hbar_j = -\dot{h}_j$. From (93), we have $\hbar_{j+1} = \dot{\hbar}_j + c_j \hbar_j = -\ddot{h}_j - c_j \dot{h}_j = -\dot{h}_{j+1}$, where we apply $\hbar_j = -\dot{h}_j$ first and (90) second, and thus, (94) holds for all $i \in \{1, \ldots, n\}$. Then, taking time derivative of (94) for $i = n$ yields $\dot{\hbar}_n = -\ddot{h}_n = -\dot{h}_{n+1} + c_n \dot{h}_n$ by (90). Then, applying (91) and (94) to this relation leads to (95).

The relation (90) with the time derivative component does not provide an explicit definition of the newly constructed CBFs h_{i+1} with respect to the formerly constructed CBFs $h_1, \ldots, h_i$. To rewrite the relation, suppose that h_{i+1} is given by

$$h_{i+1} = -p_i(t) + \alpha_i(h_1, \ldots, h_i) \tag{96}$$

where $\alpha_i(h_1, \ldots, h_i)$ is a recursive function to be determined. Then, using relation (90), and substituting (96) into the time

derivative component $\dot{h}_i$, we get

$$h_{i+1} = \dot{h}_i + c_i h_i$$

$$= -p_i(t) + \sum_{j=1}^{i-1} \frac{\partial \alpha_{i-1}}{\partial h_j}(h_{j+1} - c_j h_j) + c_i h_i. \tag{97}$$

By $h_2 = -q_c(t) + c_1 h_1$, it is clear that the initial condition of the function is $\alpha_1(h_1) = c_1 h_1$. Comparing (96) with (97), and considering $h_2 = -q_c(t) + c_1 h_1$, the function $\alpha_i(h_1, \ldots, h_i)$ is recursively solved by

$$\alpha_1(h_1) = c_1 h_1 \tag{98}$$

$$\alpha_i(h_1, \ldots, h_i) = \sum_{j=1}^{i-1} \frac{\partial \alpha_{i-1}}{\partial h_j}(h_{j+1} - c_j h_j) + c_i h_i. \tag{99}$$

Since the recursive update of $\hbar_i$ in (93) is the same as that of h_i in (90), the solution of $\hbar_i$ can also be represented by function α_i as

$$\hbar_{i+1} = p_{i+1}(t) + \sum_{j=1}^{i-1} \frac{\partial \alpha_{i-1}}{\partial \hbar_j}(\hbar_{j+1} - c_j \hbar_j) + c_i \hbar_i \tag{100}$$

where the term $p_{i+1}(t)$ in (100) is induced by the definition of $\hbar_1$ in (92).

The nonovershooting control law is designed so that (91) holds. Taking the time derivative of (96) for $i = n$ and substituting (89), to make (91) satisfied, one can obtain the nonovershooting control law as

$$U(t) = c_{n+1} h_{n+1} + \sum_{j=1}^{n} \frac{\partial \alpha_n}{\partial h_j}(h_{j+1} - c_j h_j). \tag{101}$$

Owing to Lemma 5, once we define the high-order CBFs by (91) and design the nonovershooting control to make (91) satisfied, then both (93) and (95) hold. Moreover, we require the positivity of all CBFs at $t = 0$. The properties $h_1(0) \geq 0$ and $h_2(0) \geq 0$ hold with Assumptions 2 and 3. From conditions $h_{i+1}(0) \geq 0$ for all $i \in \{1, \ldots, n\}$ and $\hbar_{i+1}(0) \geq 0$ for all $i \in \{1, \ldots, n-1\}$, and by (97) and (100), the following conditions on the gain parameters arise:

$$c_i \geq \max\{\beta_i^+(\mathbf{p}_i, \sigma_0, \mathbf{c}_{i-1}), \beta_i^-(\mathbf{p}_{i+1}, \mathbf{c}_{i-1})\} \tag{102}$$

for all $i \in \{1, \ldots, n-1\}$, and

$$c_n \geq \beta_n^+(\mathbf{p}_n, \sigma_0, \mathbf{c}_{n-1}) \tag{103}$$

where $\mathbf{p}_i = [p_1(0), p_2(0), \ldots, p_i(0)]^\top$ and $\mathbf{c}_{i-1} = [c_1, c_2, \ldots, c_{i-1}]^\top$, and the functions β_i^+ and β_i^- are defined as

$$\beta^+(\mathbf{p}_i, \sigma_0, \mathbf{c}_{i-1}) = \frac{p_i(0) - \sum_{j=1}^{i-1} \frac{\partial \alpha_{i-1}}{\partial h_j}(h_{j+1}(0) - c_j h_j(0))}{h_i(0)} \tag{104}$$
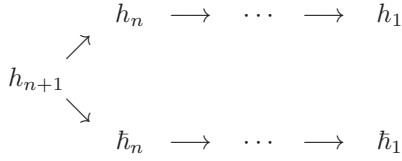
$$\beta^-(\mathbf{p}_{i+1}, \mathbf{c}_{i-1}) = \frac{p_{i+1}(0) - \sum_{j=1}^{i-1} \frac{\partial \alpha_{i-1}}{\partial \hbar_j}(\hbar_{j+1}(0) - c_j \hbar_j(0))}{\hbar_i(0)}. \tag{105}$$

Note that, while expression (104) is not explicitly written as a function with respect to $\mathbf{p}_i$ and $\mathbf{c}_{i-1}$, from the recursive formula in (99), it is clear that (104) is a function with respect to $\mathbf{p}_i$ and $\mathbf{c}_{i-1}$ once we substitute h_i by (99). An important property is that, since the lower bound condition for c_i is determined only from $\mathbf{c}_{i-1}$, the existence of the gain parameters to satisfy the conditions is ensured for sufficiently large c_i for all $i \in \{1, \dots, n\}$.

Let us now examine the chained structure (90)–(95). A clearer ordering of these $2n + 1$ subsystems is

$$\dot{h}_{n+1} = -c_{n+1} h_{n+1}$$

$$\dot{h}_n = -c_n h_n + h_{n+1}, \qquad \dot{\hslash}_n = -c_n \hslash_n + c_{n+1} h_{n+1}$$

$$\vdots \qquad\qquad\qquad\qquad \vdots$$

$$\dot{h}_1 = -c_1 h_1 + h_2, \qquad \dot{\hslash}_1 = -c_1 \hslash_1 + \hslash_2. \quad (106)$$

For even more clarity, we give the following flow diagram among these $2n + 1$ positive subsystems:

$$
\begin{array}{ccccc}
& & h_n & \longrightarrow \cdots \longrightarrow & h_1 \\
& \nearrow & & & \\
h_{n+1} & & & & \\
& \searrow & & & \\
& & \hslash_n & \longrightarrow \cdots \longrightarrow & \hslash_1
\end{array}
$$

Theorem 5: Let $s(0)$ and $T(x,0)$ satisfy Assumptions 1–3. Consider the closed-loop system (1)–(4), (6), and (87)–(89) with the nonovershooting control law (101), where the CBFs are given by (96) with the recursive update of α_i given by (98)–(99), and the gain parameters satisfy (102) for all i. Then, all CBFs defined as (11)–(14) satisfy the positivity constraints. This means, in particular, that, for all $q_c(0) \geq 0$, and for all real $p(0)$, the interface $s(t)$ does not exceed s_r, the temperature $T(x,t)$ does not drop below T_m at any position x between 0 and $s(t)$, and the heat flux $q_c(t)$ never takes a negative value. Furthermore, the closed-loop system is exponentially stable at the equilibrium $s = s_r, T(x, \cdot) \equiv 0, q_c = p = 0$, in the sense of the positive definite functional:

$$\Phi(t) := ||T[t] - T_m||^2 + (s(t) - s_r)^2 + \sum_{i=1}^{n} p_i(t)^2 \quad (107)$$

for all initial conditions in the safe set, i.e., globally. In other words, there exist positive constants $M > 0$ and $b > 0$ such that the following norm estimate holds:

$$\Phi(t) \leq M\Phi(0)e^{-bt}. \quad (108)$$

While in this section we pursued just a nonovershooting design for regulation to the barrier, it is straightforward to also design QP safety filters like in Sections IV and VI for the system with an extra integrator, treated in this section.

VIII. SAFETY FOR THE TWO-PHASE STEFAN SYSTEM UNDER DISTURBANCE

In this section, we extend the safety design to the "two-phase" Stefan problem, where the interface dynamics is affected by a heat loss modeled by the temperature dynamics in the solid
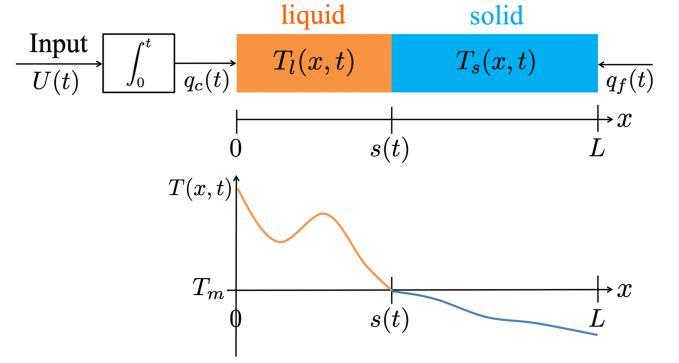

Fig. 2. Schematic of the two-phase Stefan problem with a disturbance at $x = L$.

phase. Additionally, the solid phase temperature is affected by a heat loss caused at the end boundary of the solid phase, which serves as a disturbance in the system. The safety constraint and closed-loop analysis for such a two-phase Stefan system with disturbance have been studied in [25], by means of input-to-state stability (ISS). In this article, we further incorporate the actuator dynamics, and tackle the safety verification by utilizing CBFs and nonovershooting regulation. The configuration of the two-phase Stefan problem is depicted in Fig. 2.

A. Model and Constraint

The governing equations are described by the following coupled PDE–ODE–PDE system:

$$\frac{\partial T_l}{\partial t}(x,t) = \alpha_l \frac{\partial^2 T_l}{\partial x^2}(x,t), \text{ for } t > 0, \ 0 < x < s(t) \quad (109)$$

$$\frac{\partial T_l}{\partial x}(0,t) = -q_c(t)/k_l, \ T_l(s(t),t) = T_m, \text{ for } t > 0 \quad (110)$$

$$\frac{\partial T_s}{\partial t}(x,t) = \alpha_s \frac{\partial^2 T_s}{\partial x^2}(x,t), \text{ for } t > 0, \ s(t) < x < L \quad (111)$$

$$\frac{\partial T_s}{\partial x}(L,t) = -q_f(t)/k_s, \ T_s(s(t),t) = T_m, \text{ for } t > 0 \quad (112)$$

$$\dot{q}_c(t) = U(t) \quad (113)$$

$$\gamma \dot{s}(t) = -k_l \frac{\partial T_l}{\partial x}(s(t),t) + k_s \frac{\partial T_s}{\partial x}(s(t),t) \quad (114)$$

where $\gamma = \rho_l \Delta H^*$, and all the variables denote the same physical value with the subscript "l" for the liquid phase and "s" for the solid phase. The boundary condition of the solid phase temperature given in (112) is affected by an unknown heat loss, where $q_f(t) \geq 0$ denotes the magnitude of the cooling heat flux at the side of the solid phase, which serves as a disturbance of the system. The solid phase temperature must be lower than the melting temperature, which serves as one of the conditions for the model validity. Namely, we require

$$T_l(x,t) \geq T_m \quad \forall x \in (0, s(t)) \quad \forall t > 0 \quad (115)$$

$$T_s(x,t) \leq T_m \quad \forall x \in (s(t), L) \quad \forall t > 0 \quad (116)$$

$$0 < s(t) < L \quad \forall t > 0. \quad (117)$$

The following assumption on the initial data $(T_{l,0}(x), T_{s,0}(x), s_0) := (T_l(x,0), T_s(x,0), s(0))$ is imposed.

Assumption 6: $0 < s_0 < L$, $T_{l,0}(x) \in C^0([0,s_0]; [T_m, +\infty))$, $T_{s,0}(x) \in C^0([s_0,L]; (-\infty, T_m])$, and $T_{l,0}(s_0) = T_{s,0}(s_0) = T_m$. Also, there exists constants $\bar{T}_l, \bar{T}_s, \eta_l, \eta_s > 0$ such that

$$0 \le T_{l,0}(x) - T_m \le \bar{T}_l \left(1 - \exp(L\eta_l \alpha_l^{-1}(x - s_0))\right) \quad (118)$$

for $x \in [0, s_0]$ and

$$-\bar{T}_s \left(1 - \exp(L\eta_s \alpha_s^{-1}(x - s_0))\right) \le T_{s,0}(x) - T_m \le 0 \quad (119)$$

for $x \in [s_0, L]$.

The following lemma is provided to ensure the conditions of the model validity.

Lemma 6: Let Assumption 6 hold, $q_c(t)$ and $q_f(t)$ be bounded nonnegative continuous functions $q_c \in C^0(\mathbb{R}_+; [0, \bar{q}_c))$, $q_f \in C^0(\mathbb{R}_+; [0, \bar{q}_f))$ for some $\bar{q}_c, \bar{q}_f > 0$, and

$$\max\left\{\frac{k_l \varepsilon_l}{\alpha_l}\left(1 + \frac{\alpha_l}{L^2 \eta_l}\right), \frac{k_s \varepsilon_s}{\alpha_s}\left(1 + \frac{\alpha_s}{L^2 \eta_s}\right)\right\} < \frac{\gamma}{4} \quad (120)$$

hold, where

$$\varepsilon_l := \max\left\{\bar{T}_l, \bar{q}_c L k_l^{-1}\right\}, \quad \varepsilon_s := \max\left\{\bar{T}_s, \bar{q}_f L k_s^{-1}\right\}. \quad (121)$$

Furthermore, suppose it holds

$$0 < \gamma s_\infty + \int_0^t (q_c(\tau) - q_f(\tau))\mathrm{d}\tau < \gamma L \quad (122)$$

for all $t \ge 0$, where

$$s_\infty := s_0 + \frac{k_l}{\alpha_l \gamma} \int_0^{s_0} (T_{l,0}(x) - T_m)\mathrm{d}x$$
$$+ \frac{k_s}{\alpha_s \gamma} \int_{s_0}^{L} (T_{s,0}(x) - T_m)\mathrm{d}x. \quad (123)$$

Then, there exists a unique solution to (109)–(114), which satisfies (115)–(117).

Lemma 6 is proven in [6, (Th. 1 in p. 4 and Th. 4 in p. 8)] by employing the maximum principle. The variable s_∞ is the final interface position $s_\infty = \lim_{t \to \infty} s(t)$ under the zero heat input $q_c(t) \equiv q_f(t) \equiv 0$ for all $t \ge 0$. For (122) to hold for all $t \ge 0$, we at least require it to hold at $t = 0$, which leads to the following assumption.

Assumption 7: s_∞ given by (123) satisfies $0 < s_\infty < L$.

Furthermore, we impose the restriction for the setpoint given as follows.

Assumption 8: The setpoint s_r satisfies $s_\infty < s_r < L$.

Physically, Assumption 7 states that neither phase disappears under $q_c(t) \equiv q_f(t) \equiv 0$, and Assumption 8 states that the choice of the setpoint for the melting is far beyond s_∞ from the heat input. A graphical illustration of the assumptions can be seen in Fig. 3.

B. Nonovershooting Regulation and Guaranteed Safety

Due to the addition of the solid phase temperature dynamics, the energy deficit σ in (11) is reformulated. We consider the
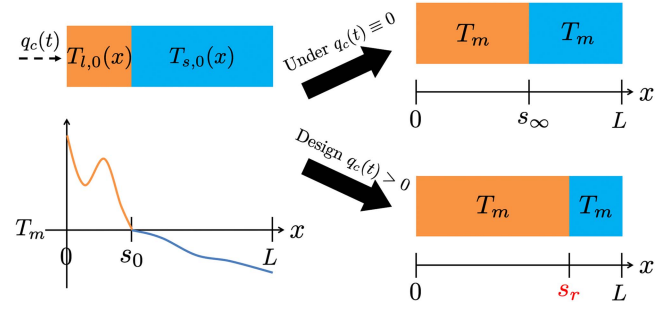

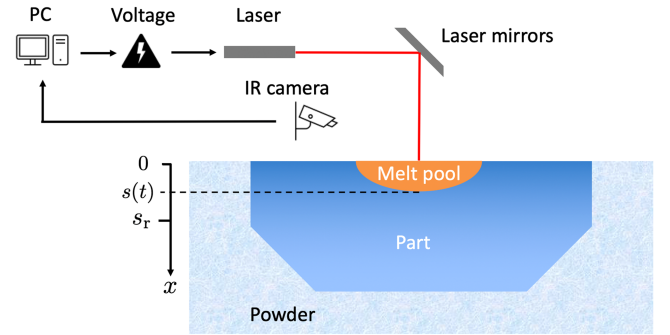Fig. 3. Graphic interpretation of s_∞ and s_r under $q_f \equiv 0$.

Fig. 4. Schematic of powder bed metal AM by selective laser sintering. The safe control should be designed to keep generating positive laser power and to avoid overshoot of the depth of melt pool beyond the desired layer thickness.

following CBFs for the two-phase problem:

$$h_1(t) := \sigma(t)$$
$$= -\left(\frac{k_l}{\alpha_l}\int_0^{s(t)}(T_l(x,t) - T_m)\mathrm{d}x\right.$$
$$\left. + \frac{k_s}{\alpha_s}\int_{s(t)}^{L}(T_s(x,t) - T_m)\mathrm{d}x + \gamma(s(t) - s_r)\right) \quad (124)$$

$$\hbar_1(t) = q_c(t) \quad (125)$$

$$h_2(t) = -q_c(t) + c_1 \sigma(t) \quad (126)$$

$$h_l(x,t) = T_l(x,t) - T_m \quad (127)$$

$$h_s(x,t) = T_m - T_s(x,t). \quad (128)$$

Then, it holds $\dot{h}_1 = -\hbar_1 + q_f(t)$, thereby the nonovershooting regulation is designed in the same manner as in Section III, which makes the following relationship to hold:

$$\dot{h}_1 = -c_1 h_1 + h_2 + q_f(t) \quad (129)$$

$$\dot{\hbar}_1 = -c_1 \hbar_1 + c_2 h_2 \quad (130)$$

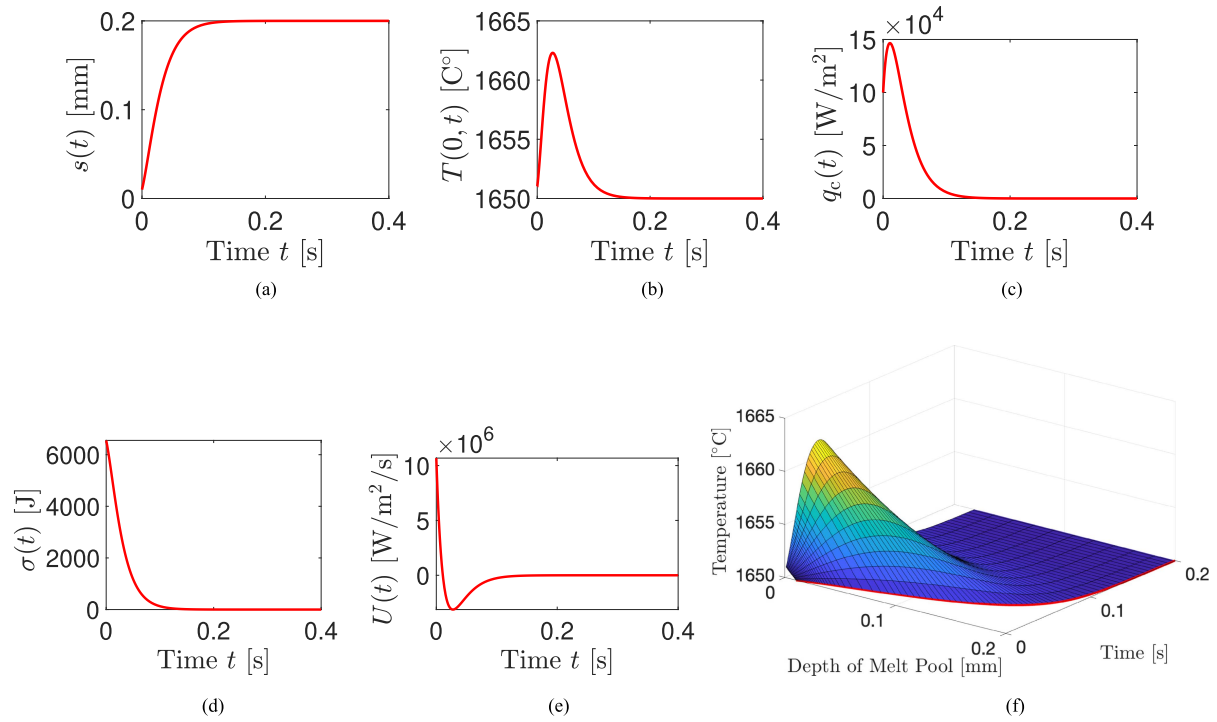$$\dot{h}_2 = -c_2 h_2 + c_1 q_f(t). \quad (131)$$

Fig. 5. Backstepping control ensures that $s(t) \to s_r$ but prevents $s(t)$ from overshooting s_r, $T(x,t)$ from undershooting T_m, and $q_c(t)$ from undershooting zero. This is achieved by nonmonotonic $q_c(t)$, which overshoots in the positive direction. (a) Interface position converges to setpoint without overshooting. (b) Liquid at the location of the laser power q_c first warms and then cools, remaining above the melting temperature 1650 °C. (c) Laser power remains positive. (d) Energy CBF remains positive. (e) Voltage input U achieves nonovershooting regulation of s. (f) Liquid temperature keeps above the melting temperature in all liquid domain.
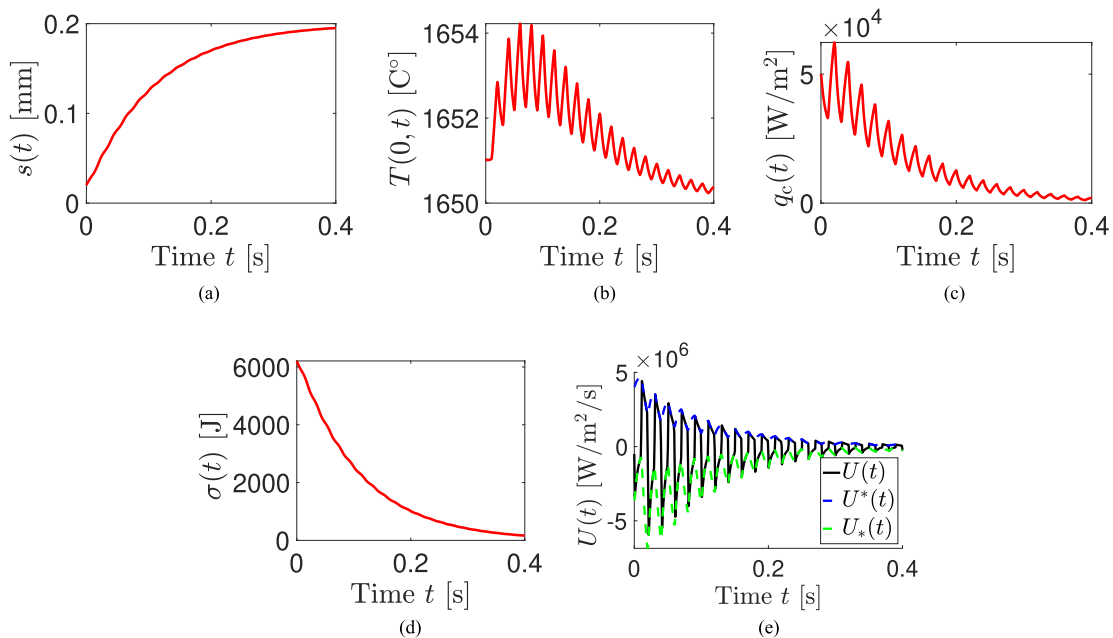

Fig. 6. Under operator input $U_o(t) = A\sin(\omega t) + B$, which commands both a periodic addition of heat and a net/average removal of heat, and would lead to islands of solid, the QP-backstepping safety input U in plot (e) ensures that the laser q_c in plot (c) remains positive, s does not exceed s_r, and T does not drop below T_m. The interface s advances because the operator periodically commands the addition of heat, in spite of the net command being for removal of heat ($B < 0$). (a) As a result of commanded heating, interface s settles to constraint s_r. (b) Temperature adjacent to heat flux q_c fluctuates but remains above melting. (c) Inlet heat flux fluctuates but remains positive—it never cools. (d) Energy CBF remains positive. (e) QP-backstepping voltage input is kept between the lower and upper bounds.

Namely, the nonovershooting regulation is designed as

$$U^*(\sigma, q_c) = -(c_1 + c_2)q_c + c_1 c_2 \sigma. \qquad (132)$$

To satisfy inequality (120), we impose the following assumption.

Assumption 9: $q_f(t) \in C^0(\mathbb{R}_+; [0, \bar{q}_f))$ for some $\bar{q}_f > 0$ satisfying

$$\bar{q}_f < \min \left\{ q_c(0) + c_1 \gamma s_\infty, \frac{c_1 c_2}{c_1 + c_2} \gamma s_r \right\} \qquad (133)$$

and inequality (120) holds with

$$\bar{q}_c = \max \left\{ q_c(0), \frac{c_2}{c_1}(c_1 \sigma(0) - q_c(0)), \bar{q}_f \right\}. \qquad (134)$$

With $q_f \geq 0$ in Assumption 9, and with the gain condition

$$c_1 \geq \frac{q_c(0)}{\sigma(0)} \qquad (135)$$

relationship (129)–(131) leads to

$$h_1 \geq 0, \quad \hbar_1 \geq 0, \quad h_2 \geq 0. \qquad (136)$$

Moreover, in the same manner as in Section VI, an upper bound of the solution to (129)–(131) is also obtained, which ensures that $q_c(t) \leq \bar{q}_c$. Therefore, with Assumption 9, condition (120) is satisfied.

It remains to ensure condition (122). Taking the time integration to the relation $\dot{h}_1 = -q_c(t) + q_f(t)$, and by $h_1(0) = \gamma s_r - \gamma s_\infty$, one can obtain

$$\gamma s_\infty + \int_0^t (q_c(\tau) - q_f(\tau)) d\tau = \gamma s_r - h_1(t). \qquad (137)$$

Since $h_1 \geq 0$ is already ensured, with Assumption 8, the right inequality in (122) is satisfied. Moreover, by relation (129)–(131), the upper bound of h_1 is shown as

$$h_1(t) \leq \max \left\{ h_1(0), \frac{1}{c_1} \left(\max \left\{ h_2(0), \frac{c_1}{c_2} \bar{q}_f \right\} + \bar{q}_f \right) \right\}. \qquad (138)$$

Hence, with (133) in Assumption 9, one can deduce that the left inequality in (122) is also satisfied. Thus, applying Lemma 6, the safety constraint (115)–(115) is satisfied under the nonovershooting design in (132). We state the following theorem.

Theorem 6: Let $s(0)$ and $T_l(x, 0)$, and $T_s(x, 0)$ satisfy Assumption 6–8, and $q_f(t)$ satisfy Assumption 9. Consider the closed-loop system (109)–(114) with the nonovershooting control law (132), where the gain parameters satisfy (135) and $c_2 \geq 0$. Then, all CBFs defined as (124)–(128) satisfy the positivity constraints. This means, in particular, that, for all $q_c(0) > 0$, the interface $s(t)$ remains inside $(0, L)$, the liquid temperature $T_l(x, t)$ does not drop below T_m at any position x between 0 and $s(t)$, the solid temperature $T_s(x, t)$ does not go above T_m at any position x between $s(t)$ and L, and the heat flux $q_c(t)$ never takes a negative value. Furthermore, the closed-loop system is exponentially ISS at the equilibrium $s = s_r, T_l(x, \cdot) \equiv T_m, T_s(x, \cdot) \equiv T_m, q_c = 0$, in the sense of the following positive definite functional:

$$\Phi(t) := ||T_l[t] - T_m||^2 + ||T_s[t] - T_m||^2 + (s(t) - s_r)^2 + q_c(t)^2 \qquad (139)$$

Description	Symbol	Value
Density	ρ	$3920 \text{ kg} \cdot \text{m}^{-3}$
Latent heat of fusion	$\triangle H^*$	$2.86 \times 10^5 \text{ J} \cdot \text{kg}^{-1}$
Heat Capacity	C_p	$830 \text{ J} \cdot \text{kg}^{-1} \cdot {}^\circ\text{C}^{-1}$
Thermal conductivity	k	$32.5 \text{ W} \cdot \text{m}^{-1}$
Melting temperature	T_m	$1650 \,{}^\circ\text{C}$

for all initial conditions in the safe set, i.e., globally. In other words, there exist positive constants $M_1 > 0$, $M_2 > 0$, and $b > 0$ such that the following estimate holds:

$$\Phi(t) \leq M_1 \Phi(0) e^{-bt} + M_2 \sup_{\tau \in [0,t]} q_f(\tau). \qquad (140)$$

The safety is already proven in this section. The ISS proof is identical to the steps performed in [25, Sec. 5-2], which is omitted in this article.

IX. APPLICATION TO AM

We apply the safe control methods proposed in Sections III and IV to metal AM with selective laser sintering, which has been intensively advanced in the recent decade as observed from the growth in global market [8]. The Stefan model describes the expansion of melt pool inside the powder bed, which is generated by laser input [46]. We consider controlling the voltage input, which manipulates the laser power, for the sake of obtaining the desired depth of the melt pool, which is a thickness of layer. The safe set is the positivity of the laser power and the energy deficit for avoiding the overshooting of the melt pool deeper than the desired thickness. The schematic of the metal AM is depicted in Fig. 4.

We perform the numerical simulation considering a titanium alloy (Ti6Al4V), the physical parameters of which are given in Table I. The 1-D Stefan model is numerically computed by the well-known boundary immobilization method combined with finite difference semidiscretization [34].

First, we investigate the performance of the nonovershooting control law (45). The initial depth of the melt pool is set to $s_0 = 0.01$ [mm], and the initial temperature profile is set to a linear profile $T_0(x) = \bar{T}(1 - x/s_0) + T_m$ with $\bar{T} = 1 \,[^\circ\text{C}]$. The setpoint position is set as $s_r = 0.2$ [mm], which is a reasonable value for layer thickness in metal AM. The control gains are set as $k_1 = 8q_c(0)/\sigma(0) = 64.4$ [/s], $k_2 = 973$ [/s^2]. Fig. 5 depicts the result of the closed-loop response. Fig. 5(a) illustrates that the melt pool depth successfully converges to the setpoint monotonically without overshooting, namely, the regulation is achieved. Fig. 5(b) shows that the surface temperature of the melt pool is warmed up first and cooled down once the heat is sufficiently added, with maintaining above the melting temperature. Fig. 5(c) and (d) depict the two CBFs imposed in the problem, one for an energy deficit and the other for a laser power, both of which satisfy the positivity condition. Fig. 5(e) shows the voltage input which does not have any constraint under the nonovershooting control. Fig. 5(f) shows 3-D surface plot of the temperature profile in the liquid melt pool, which remains above the melting temperature in all the liquid domain. Hence, the numerical result

is consistent with Theorem 2 on nonovershooting control in terms of achieving stabilization and safety simultaneously.

Next, we conduct the simulation of the QP-backstepping safety control (44), with lower bound (37) and upper bound (38). We set the operator input as $U_o(t) = A\sin(\omega t) + B$, where $A = 1.14 \times 10^7$, $B = -5 \times 10^5$, and $\omega = 2\pi/\tau$ with time period $\tau = 0.02$ [s]. The control gains are set as $k_1 = 64.4$ [/s], $k_2 = 973$ [/s^2], $\delta_1 = 129$ [/s], and $\delta_2 = 195$ [/s^2], respectively. Fig. 6 depicts the result of the closed-loop response. Fig. 6(a) illustrates that the interface position monotonically increases with maintaining $s(t) < s_r$, and slowly converges to the setpoint position. Fig. 6(b) shows QP-backstepping voltage input (black solid), the lower bound (green dash), and the upper bound (blue dash). We observe that the input is affected by both the upper and lower bounds, to maintain the value between them, while it executes the operator input other than that, which is a sinusoidal wave input. We can also see that, as time passes, the lower bound gradually corresponds to the upper bound, as well as the QP input, thereby the regulation of the interface position can be achieved slowly in Fig. 6(a). Due to the operator input, Fig. 6 shows that the boundary temperature is fluctuating through repeating the warming up and cooling down, with maintaining above the melting temperature. Similar behavior can be observed in Fig. 6(e) showing the laser power. Also in this setup, as observed in Fig. 5(d) and (e), the two CBFs imposed in the problem satisfy the positivity, which ensures the desired performance of the safety filter, being consistent with Theorem 1.

X. CONCLUSION

This article has developed two safe control strategies for the one-phase Stefan PDE–ODE system with actuator dynamics by utilizing CBF. The first one is the nonovershooting control, which is derived by the recursive construction of CBFs for ensuring the safety imposed by the physical model, and also achieves the regulation of the moving interface position at a desired setpoint position. The second one is the safety filter design, which employs an operator input under the conditions of maintaining safety, as a QP-backstepping-CBF formulation. The stability proof under the nonovershooting control has been achieved by PDE-backstepping method and Lyapunov analysis. The developed methods have been extended to the case of additional constraints from above on the states, the system with higher order actuator dynamics, and the two-phase Stefan system with an unknown disturbance. The proposed nonovershooting control and the QP safety filter design have been demonstrated in numerical simulation of the process in metal AM, which illustrates the desired performance. Namely, both regulation and safety are simultaneously achieved by the nonovershooting control, while the safety filter affects the system by a chosen operator input with maintaining safety.

APPENDIX A
DERIVATION OF ACTUATOR DYNAMICS

We consider that the true voltage input $V_{in}(t)$ is connected to RC series circuit whose opposite side has a heater with the heat flux $q_c(t)$ and the voltage $V_c(t)$. The relation between the power

and the voltage is given by

$$Aq_c(t) = \frac{V_c(t)^2}{R_c} \tag{141}$$

where A is a surface area of the material, and R_c is a resistance of the heater. The circuit equation of the first-order RC series satisfies

$$RC\dot{V}_c(t) + V_c(t) = V_{in}(t). \tag{142}$$

Taking the time-derivative of (141) leads to

$$\dot{q}_c(t) = \frac{2V_c(t)}{AR_c RC}\left(-V_c(t) + V_{in}(t)\right). \tag{143}$$

Therefore, by defining $U(t)$ as

$$U(t) = \frac{2V_c(t)}{AR_c RC}\left(-V_c(t) + V_{in}(t)\right) \tag{144}$$

we have

$$\dot{q}_c(t) = U(t). \tag{145}$$

Higher order actuator dynamics in Section VII can be modeled in a similar manner by considering higher order RC series circuit.

REFERENCES

[1] V. Alexiades and A. D. Solomon, *Mathematical Modeling of Melting and Freezing Processes*. Evanston, IL, USA: Routledge, 2018.

[2] A. D. Ames, X. Xu, J. W. Grizzle, and P. Tabuada, "Control barrier function based quadratic programs for safety critical systems," *IEEE Trans. Autom. Control*, vol. 62, no. 8, pp. 3861–3876, Aug. 2017.

[3] A. Armaou and P. D. Christofides, "Robust control of parabolic PDE systems with time-dependent spatial domains," *Automatica*, vol. 37, no. 1, pp. 61–69, 2001.

[4] S. Bansal, M. Chen, S. Herbert, and C. J. Tomlin, "Hamilton-Jacobi reachability: A brief overview and recent advances," in *Proc. 56th IEEE Annu. Conf. Decis. Control*, 2017, pp. 2242–2253.

[5] J. Breeden and D. Panagou, "High relative degree control barrier functions under input constraints," in *Proc. IEEE 60th Conf. Decis. Control*, 2021, pp. 6119–6124.

[6] J. R. Cannon and M. Primicerio, "A two phase Stefan problem with flux boundary conditions," *Annali diMatematicaPuraed Applicata*, vol. 88, no. 1, pp. 193–205, 1971.

[7] X.-F. Chen, J. Chadam, L.-S. Jiang, and W. Zheng, "Convexity of the exercise boundary of the American put option on a zero dividend asset," *Math. Finance: An Int. J. Math., Statist. Financial Econ.*, vol. 18, no. 1, pp. 185–197, 2008.

[8] M. Cotteleer and J. Joyce, "3D opportunity: Additive manufacturing paths to performance, innovation, and growth," *Deloitte Rev.*, vol. 14, pp. 5–19, 2014.

[9] N. Daraoui, P. Dufour, H. Hammouri, and A. Hottot, "Model predictive control during the primary drying stage of lyophilisation," *Control Eng. Pract.*, vol. 18, no. 5, pp. 483–494, 2010.

[10] C. Demir, S. Koga, and M. Krstic, "Neuron growth control by PDE backstepping: Axon length regulation by tubulin flux actuation in soma," in *Proc. IEEE 60th Conf. Decis. Control*, 2021, pp. 649–654.

[11] V. Dhiman, M. Javad Khojasteh, M. Franceschetti, and N. Atanasov, "Control barriers in Bayesian learning of system dynamics," *IEEE Trans. Autom. Control*, vol. 68, no. 1, pp. 214–229, Jan. 2023.

[12] Y. Du and Z. Lin, "Spreading-vanishing dichotomy in the diffusive logistic model with a free boundary," *SIAM J. Math. Anal.*, vol. 42, no. 1, pp. 377–405, 2010.

[13] W. B. Dunbar, N. Petit, P. Rouchon, and P. A. Martin, "Motion planning for a nonlinear Stefan problem," *ESAIM: Control Optim. Calculus Variations*, vol. 9, pp. 275–296, 2003.

[14] S. Ecklebe, F. Woittennek, C. Frank-Rotsch, N. Dropka, and J. Winkler, "Toward model-based control of the vertical gradient freeze crystal growth process," *IEEE Trans. Control Syst. Technol.*, vol. 30, no. 1, pp. 384–391, Jan. 2022.

[15] A. Friedman and F. Reitich, "Analysis of a mathematical model for the growth of tumors," *J. Math. Biol.*, vol. 38, no. 3, pp. 262–284, 1999.

[16] S. C. Gupta, *The Classical Stefan Problem: Basic Concepts, Modelling and Analysis With Quasi-Analytical Solutions and Methods*, vol. 45. Amsterdam, Netherlands: Elsevier, 2017.

[17] L. Hewing, K. P. Wabersich, M. Menner, and M. N. Zeilinger, "Learning-based model predictive control: Toward safe learning in control," *Annu. Rev. Control Robot. Auton. Syst.*, vol. 3, pp. 269–296, 2020.

[18] C. Hill, "Parabolic equations in one space variable and the non-characteristic cauchy problem," *Commun. Pure Appl. Math.*, vol. 20, pp. 619–633, 1967.

[19] I. Karafyllis and M. Krstic, "Stability of integral delay equations and stabilization of age-structured models," *ESAIM: COCV*, vol. 23, no. 4, pp. 1667–1714, 2017.

[20] M. Jankovic, "Robust control barrier functions for constrained stabilization of nonlinear systems," *Automatica*, vol. 96, pp. 359–367, 2018.

[21] I. Karafyllis and M. Krstic, "Global stabilization of compressible flow between two moving pistons," *SIAM J. Control Optim.*, vol. 60, no. 2, pp. 1117–1142, 2021.

[22] I. Karafyllis and M. Krstic, "Spill-free transfer and stabilization of viscous liquid," *IEEE Trans. Autom. Control*, vol. 67, no. 9, pp. 4585–4597, Sep. 2022.

[23] S. Koga, L. Camacho-Solorio, and M. Krstic, "State estimation for lithium-ion batteries with phase transition materials via boundary observers," *J. Dyn. Syst. Meas. Control*, vol. 143, no. 4, 2021, Art. no. 041004.

[24] S. Koga, M. Diagne, and M. Krstic, "Control and state estimation of the one-phase Stefan problem via backstepping design," *IEEE Trans. Autom. Control*, vol. 64, no. 2, pp. 510–525, Feb. 2019.

[25] S. Koga, I. Karafyllis, and M. Krstic, "Towards implementation of PDE control for Stefan system: Input-to-state stability and sampled-data design," *Automatica*, vol. 127, 2021, Art. no. 109538.

[26] S. Koga and M. Krstic, "Arctic sea ice state estimation from thermodynamic PDE model," *Automatica*, vol. 112, 2020, Art. no. 108713.

[27] S. Koga and M. Krstic, *Materials Phase Change PDE Control and Estimation: From Additive Manufacturing to Polar Ice*. Berlin, Germany: Springer Nature, 2020.

[28] S. Koga and M. Krstic, "Safe PDE backstepping QP control with high relative degree CBFs: Stefan model with actuator dynamics," in *Proc. IEEE Amer. Control Conf.*, 2022, pp. 2033–2038.

[29] S. Koga, M. Krstic, and J. Beaman, "Laser sintering control for metal additive manufacturing by PDE backstepping," *IEEE Trans. Control Syst. Technol.*, vol. 28, no. 5, pp. 1928–1939, Sep. 2020.

[30] S. Koga, M. Makihata, R. Chen, M. Krstic, and A. P. Pisano, "Energy storage in paraffin: A PDE backstepping experiment," *IEEE Trans. Control Syst. Technol.*, vol. 29, no. 4, pp. 1490–1502, Jul. 2021.

[31] M. Krstic, *Delay Compensation for Nonlinear, Adaptive, and PDE Systems*. Berlin, Germany: Springer, 2009.

[32] M. Krstic and M. Bement, "Nonovershooting control of strict-feedback nonlinear systems," *IEEE Trans. Autom. Control*, vol. 51, no. 12, pp. 1938–1943, Dec. 2006.

[33] M. Krstic and A. Smyshlyaev, *Boundary Control of PDEs: A Course on Backstepping Designs*. Philadelphia, PA, USA: SIAM, 2008.

[34] S. Kutluay, A. R. Bahadir, and A. Özdeş, "The numerical solution of one-phase classical Stefan problem," *J. Comput. Appl. Math.*, vol. 81, no. 1, pp. 135–144, 1997.

[35] A. Maidi and J. P. Corriou, "Boundary geometric control of a linear Stefan problem," *J. Process Control*, vol. 24, no. 6, pp. 939–946, 2014.

[36] L. J. McGilly, P. Yudin, L. Feigl, A. K. Tagantsev, and N. Setter, "Controlling domain wall motion in ferroelectric thin films," *Nature Nanotechnol.*, vol. 10, no. 2, pp. 145–150, 2015.

[37] K. C. Mills, *Recommended Values of Thermophysical Properties for Selected Commercial Alloys*. Sawston, U.K.: Woodhead Publishing, 2002.

[38] Q. Nguyen and K. Sreenath, "Exponential control barrier functions for enforcing high relative-degree safety-critical constraints," in *Proc. IEEE Amer. Control Conf.*, 2016, pp. 322–328.

[39] B. Petrus, J. Bentsman, and B. G. Thomas, "Enthalpy-based feedback control algorithms for the Stefan problem," in *Proc. IEEE 51st Conf. Decis. Control*, 2012, pp. 7037–7042.

[40] Y. Rabin and A. Shitzer, "Numerical solution of the multidimensional freezing problem during cryosurgery," *J. Biomechanical Eng.*, vol. 120, no. 1, pp. 32–37, 1998.

[41] S. Singh, A. Majumdar, J. J. Slotine, and M. Pavone, "Robust online motion planning via contraction theory and convex optimization," in *Proc. IEEE Int. Conf. Robot. Autom.*, 2017, pp. 5883–5890.

[42] A. Smyshlyaev and M. Krstic, "Closed-form boundary state feedbacks for a class of 1-D partial integro-differential equations," *IEEE Trans. Autom. Control*, vol. 49, no. 12, pp. 2185–2202, Dec. 2004.

[43] H. Wang, F. Wang, and K. Xu, *Modeling Information Diffusion in Online Social Networks With Partial Differential Equations*, vol. 7. Berlin, Germany: Springer, 2020.

[44] W. Xiao and C. Belta, "Control barrier functions for systems with high relative degree," in *Proc. IEEE 58th Conf. Decis. Control*, 2019, pp. 474–479.

[45] X. Xu, "Constrained control of input–output linearizable systems using control sharing barrier functions," *Automatica*, vol. 87, pp. 195–201, 2018.

[46] K. Zeng, D. Pal, and B. Stucker, "A review of thermal analysis methods in laser sintering and selective laser melting," in *Proc. Solid Freeform Fabr. Symp.*, 2012, pp. 796–814.

Shumon Koga (Member, IEEE) received the B.S. degree in applied physics from Keio University, Tokyo, Japan, in 2014, and the M.S. and Ph.D. degrees in mechanical and aerospace engineering from the University of California, San Diego, La Jolla, CA, USA, in 2016 and 2020, respectively.

He was an intern at NASA Jet Propulsion Laboratory (USA) and Mitsubishi Electric Research Laboratories (USA), during the fall of 2017 and the summer of 2018, respectively. He is currently a Postdoctoral Researcher with Existential Robotics Laboratory in Electrical and Computer Engineering, University of California, San Diego. His doctoral research interests include distributed parameter systems, optimization by extremum seeking, and their applications to additive manufacturing, battery management, thermal management in buildings, transportation systems, and global climate systems. His current research interests include optimization and machine learning for robotics, in particular, simultaneous localization and mapping (SLAM), path planning, and safety-critical systems.

Dr. Koga was the recipient of the Robert E. Skelton Systems and Control Dissertation Award from UC San Diego Center for Control Systems and Dynamics in 2020, the O. Hugo Schuck Best Paper Award from American Automatic Control Council in 2019, and the Outstanding Graduate Student Award in Mechanical and Aerospace Engineering from UC San Diego in 2018.

Miroslav Krstic (Fellow, IEEE) received the B.S. degree in electrical engineering from the University of Belgrade, Belgrade, Yugoslavia, in 1989, and the M.S. and Ph.D. degrees in electrical and computer engineering from the University of California, Santa Barbara, CA, USA, in 1992 and 1994, respectively.

He is currently a Distinguished Professor of Mechanical and Aerospace Engineering, holds the Alspach Endowed Chair, and is the founding Director of the Cymer Center for Control Systems and Dynamics at UC San Diego (UCSD), La Jolla, CA, USA. He is also a Senior Associate Vice Chancellor for Research at UCSD. He was editor of two Springer book series. He has coauthored 15 books on adaptive, nonlinear, and stochastic control, extremum seeking, control of PDE systems including turbulent flows, and control of delay systems.

Prof. Krstic, as a graduate student, was the recipient of the UC Santa Barbara Best Dissertation Award and Student Best Paper awards at CDC and ACC. He has been an elected Fellow of six scientific societies—IFAC, ASME, SIAM, AAAS, IET (U.K.), and AIAA (Assoc. Fellow)—and as a Foreign Member of the Serbian Academy of Sciences and Arts and of the Academy of Engineering of Serbia. He was also the recipient of the Richard E. Bellman Control Heritage Award, SIAM Reid Prize, ASME Oldenburger Medal, Nyquist Lecture Prize, Paynter Outstanding Investigator Award, Ragazzini Education Award, IFAC Nonlinear Control Systems Award, Chestnut Textbook Prize, Control Systems Society Distinguished Member Award, the PECASE, NSF Career, and ONR Young Investigator Awards, the Schuck ('96 and '19) and Axelby Paper Prizes, and the First UCSD Research Award given to an engineer. He has also been awarded the Springer Visiting Professorship at UC Berkeley, the Distinguished Visiting Fellowship of the Royal Academy of Engineering, the Invitation Fellowship of the Japan Society for the Promotion of Science, and four honorary professorships outside of the United States. He is the Editor-in-Chief of *Systems & Control Letters* and has been a Senior Editor of *Automatica* and IEEE TRANSACTIONS ON AUTOMATIC CONTROL, and was the Vice President for Technical Activities of the IEEE Control Systems Society and the Chair of the IEEE CSS Fellow Committee.